ELMİ İŞ Beynəlxalq Elmi Jurnal. İyun 2026, Cild: 20, Sayı: 4, s. 336–358
SCIENTIFIC WORK International Scientific Journal. June 2026, Volume: 20, Issue: 4, pp. 336–358
DOI: https://doi.org/10.36719/2663-4619/128/336-358

Development and Experimental Evaluation of a Frequency-Hopping-Based Control and Telemetry System for Unmanned Aerial Vehicles Under Radio-Electronic Warfare Conditions

Muxtar Azizullayev[1*], Rashad Nematzade[2], Gunel Rzayeva[3], Turkan Muradova[4], Nuray Azizullayeva[4]

Abstract: *This study examines a frequency hopping-based communication approach aimed at improving the reliability of unmanned aerial vehicle (UAV) telemetry systems under radio-electronic warfare conditions. Within the framework of the research, a flight controller based on the STM32 F405 microcontroller was designed in the EasyEDA environment, and two alternative telemetry communication configurations were implemented on the same hardware platform. In the first configuration, the NRF24L01 module was employed for communication in the 2.4 GHz band, whereas in the second configuration, the RFD868x module operating in the 868 MHz band was integrated and evaluated under identical test conditions. To enhance resistance against interference and channel blocking, a frequency hopping algorithm was developed and incorporated into the telemetry architecture. Experimental investigations were carried out at distances of 50 m, 100 m, 200 m, and 500 m in order to assess the communication performance of both configurations. During the tests, key transmission parameters, including RSSI, SNR, BER, latency, and Path Loss, were measured and interpreted together with the corresponding mathematical models. The results indicate that the proposed frequency hopping approach significantly increases telemetry channel resilience in the presence of radio-electronic interference. In addition, the comparative analysis confirms that communication stability depends not only on the hopping strategy itself, but also on the selected frequency band, telemetry module characteristics, and antenna configuration.*

Keywords: *unmanned aerial vehicle (UAV), telemetry system, frequency hopping, FHSS, radio-electronic warfare, electromagnetic interference, signal-to-noise ratio (SNR), received signal strength indicator (RSSI), bit error rate (BER), path loss, telemetry channel, communication reliability, flight controller, anti-jamming communication, wireless telemetry*

[1]Azerbaijan Technical University, PhD student, Baku, Azerbaijan
[2]Baku, Azerbaijan
[3]Institute of Scientific Research Aerospace Informatics of NASA, Baku, Azerbaijan
[4]Azerbaijan Technical University, bachelor, Baku, Azerbaijan
[*]Corresponding author. E-mail: mukhtar.azizullayev@aztu.edu.az
Received: 5 March 2026; Accepted: 20 May 2026; Published online: 22 June 2026

Radioelektron mübarizə şəraitində pilotsuz uçuş aparatlarının idarə olunması və telemetrik məlumat ötürülməsi üçün tezlik sıçrayışlı sistemin işlənib hazırlanması və eksperimental sınaqları

Muxtar Əzizullayev[1*], Rəşad Nemətzadə[2], Günel Rzayeva[3], Türkan Muradova[4], Nuray Əzizullayeva[4]

Xülasə: *Bu tədqiqat radioelektron mübarizə şəraitində pilotsuz uçuş aparatlarının (PUA) telemetriya sistemlərinin etibarlılığının artırılmasına yönəlmiş tezlik sıçrayışına əsaslanan rabitə yanaşmasını araşdırır. Tədqiqat çərçivəsində EasyEDA mühitində STM32 F405 mikroidarəedicisi əsasında uçuş kontrolleri layihələndirilmiş və eyni aparat platformasında iki alternativ telemetriya rabitə konfiqurasiyası həyata keçirilmişdir. Birinci konfiqurasiyada 2,4 GHz diapazonunda rabitə üçün NRF24L01 modulu istifadə edilmiş, ikinci konfiqurasiyada isə 868 MHz diapazonunda fəaliyyət göstərən RFD868x modulu inteqrasiya olunmuş və eyni sınaq şərtləri altında qiymətləndirilmişdir. Müdaxilələrə və kanalın bloklanmasına qarşı dayanıqlığın artırılması məqsədilə tezlik sıçrayışı alqoritmi hazırlanmış və telemetriya arxitekturasına inteqrasiya edilmişdir. Hər iki konfiqurasiyanın rabitə göstəricilərini qiymətləndirmək üçün 50 m, 100 m, 200 m və 500 m məsafələrdə eksperimental tədqiqatlar aparılmışdır. Sınaqlar zamanı RSSI, SNR, BER, gecikmə (latency) və yol itkisi (Path Loss) kimi əsas ötürmə parametrləri ölçülmüş və müvafiq riyazi modellərlə birlikdə təhlil edilmişdir. Nəticələr göstərir ki, təklif olunan tezlik sıçrayışı yanaşması radioelektron müdaxilələrin mövcud olduğu şəraitdə telemetriya kanalının dayanıqlığını əhəmiyyətli dərəcədə artırır. Bundan əlavə, müqayisəli təhlil təsdiq edir ki, rabitənin sabitliyi yalnız tezlik sıçrayışı strategiyasından deyil, həm də seçilmiş tezlik diapazonundan, telemetriya modulunun xüsusiyyətlərindən və antenna konfiqurasiyasından asılıdır.*

Açar sözlər: *pilotsuz uçuş aparatı (PUA), telemetriya sistemi, tezlik sıçrayışı, FHSS, radioelektron mübarizə, elektromaqnit müdaxiləsi, siqnal-küy nisbəti (SNR), qəbul edilmiş siqnal gücü göstəricisi (RSSI), bit səhv əmsalı (BER), yol itkisi (Path Loss), telemetriya kanalı, rabitənin etibarlılığı, uçuş kontrolleri, müdaxiləyə davamlı rabitə, simsiz telemetriya*

---

[1]Azərbaycan Texniki Universiteti, doktorant, Bakı, Azərbaycan
[2]Bakı, Azərbaycan
[3]MAKA-nın Elmi Tədqiqat Aerokosmik İnformatika İnstitutu, Bakı, Azərbaycan
[4]Azərbaycan Texniki Universiteti, bakalavr, Bakı, Azərbaycan
[*]Məsul müəllif. E-poçt: mukhtar.azizullayev@aztu.edu.az
Daxil oldu: 5 Mart 2026; Qəbul edildi: 20 May 2026; Onlayn dərc edildi: 22 İyun 2026

Introduction

In recent years, unmanned aerial vehicles (UAVs) have been widely used in military, civil, industrial, and monitoring applications due to their mobility, rapid deployment, and multifunctional capabilities. The operational efficiency of UAVs strongly depends on the reliability of telemetry and control links, which ensure real-time data exchange between the onboard system and the ground station. Under radio-electronic warfare (REW) conditions, these links may be degraded by signal attenuation, noise, and intentional electromagnetic interference, resulting in data loss, increased latency, and reduced signal quality (Azizullayev & Nematzade, 2025; Aghayev et al., 2025).

Similar reliability challenges are also observed in other unmanned platforms, including unmanned surface vehicles and intelligent autonomous systems, where communication resilience, situational awareness, and operational stability are critical for mission performance (Rustamov et al., 2025).

Fixed-frequency telemetry channels are particularly vulnerable to detection, suppression, and jamming in hostile electromagnetic environments. Frequency-Hopping Spread Spectrum (FHSS) is considered an effective anti-jamming method because it changes the carrier frequency according to a pseudo-random sequence and reduces the probability of continuous interference on a single channel (Rüstəmov et al., 2023; Rustamov et al., 2024). Telemetry reliability depends not only on the communication protocol, but also on operating frequency, antenna characteristics, and module design (Rustamov et al., 2025; Ghouz et al., 2020).

In this study, an FHSS-based telemetry approach is investigated using an STM32 F405-based flight controller designed in the EasyEDA environment. Two telemetry configurations are compared: NRF24L01 operating in the 2.4 GHz band and RFD868x operating in the 868 MHz band. Their performance is evaluated at distances of 50 m, 100 m, 200 m, and 500 m using RSSI, SNR, effective SNR, SINR, BER, latency, and path loss indicators. The scientific contribution of this paper is the integrated evaluation of an STM32 F405-based UAV telemetry architecture, FHSS-based communication, two telemetry modules operating in different frequency bands, antenna radiation characteristics, and mathematical channel models within a unified framework.

Recent studies show that UAV telemetry reliability is a key factor affecting mission continuity, flight safety, and operational stability under radio-electronic warfare conditions. Telemetry channels are mainly degraded by propagation loss, external noise, intentional interference, and jamming due to limited transmission power, compact antennas, and variable flight conditions (Azizullayev & Nematzade, 2025; Aghayev et al., 2025). Telemetry degradation is usually reflected in reduced received signal strength indicator (RSSI), signal-to-noise ratio (SNR), signal-to-interference-plus-noise ratio (SINR), and packet delivery ratio (PDR), while bit error rate (BER), packet loss ratio (PLR), path loss, and latency increase with distance and interference intensity. Therefore, these indicators are widely used to evaluate telemetry reliability under interference-affected conditions (Rustamov et al., 2025; Yang et al., 2025).

Fixed-frequency telemetry systems are vulnerable to detection, suppression, and channel blocking. FHSS is widely applied as an anti-jamming method because it changes the operating frequency according to a pseudo-random sequence and reduces the probability of continuous interference on a single carrier. However, its effectiveness depends on the selected frequency band, receiver sensitivity, antenna gain, transmission power, and module characteristics (Rüstəmov et al., 2023; Zidane et al., 2024).

The operating frequency band also affects telemetry reliability. NRF24L01 modules operating at 2.4 GHz are suitable for compact UAV platforms and short-range low-latency telemetry, but this band is more sensitive to path loss and interference. In contrast, sub-GHz systems such as RFD868x at 868 MHz generally provide lower path loss, better propagation stability, and stronger signal quality over longer distances (Azizullayev, 2025; Rustamov et al., 2024). Flight controller and antenna design are also important for reliable telemetry integration. STM32 F405-based controllers provide sufficient processing capability and interfaces such as UART, SPI, and I2C for integrating different telemetry modules. In addition, antenna gain, radiation pattern, and directional energy distribution directly affect RSSI, SNR, SINR, and link stability (Rustamov et al., 2025; Ghouz et al., 2020).

Despite existing studies on UAV telemetry and anti-jamming communication, many works focus on only one module, one frequency band, or one performance indicator. Therefore, this study evaluates NRF24L01 and RFD868x telemetry configurations on the same STM32 F405-based UAV flight

controller platform using FHSS-based communication, mathematical modeling, antenna radiation analysis, and comparative performance indicators.

Methods

This study evaluates the performance and reliability of UAV telemetry systems under radio-electronic warfare (REW) conditions. Since telemetry channels operate in dynamic electromagnetic environments, their quality was assessed using RSSI, SNR, SINR, BER, path loss, and latency, which are commonly applied to analyze wireless links affected by interference and signal degradation (Azizullayev & Nematzade, 2025; Rustamov et al., 2025). RSSI characterizes the received signal level, SNR reflects the ratio between useful signal and noise, SINR accounts for both noise and interference, BER indicates transmission error probability, path loss describes distance-dependent attenuation, and latency represents transmission delay (Heydərov & Əzizullayev, 2024). Under REW conditions, fixed-frequency telemetry channels are vulnerable to jamming; therefore, FHSS was applied to improve communication robustness by switching the carrier frequency according to a pseudo-random sequence (Rüstəmov et al., 2023; Zidane et al., 2024).

3.1. Proposed UAV System Architecture. The proposed telemetry system was implemented on an STM32 F405-based flight controller. Two telemetry configurations were evaluated under identical operating conditions: NRF24L01 in the 2.4 GHz band for short-range low-latency communication, and RFD868x in the 868 MHz band for more stable long-range telemetry transmission. This structure enables the comparative assessment of frequency band, module characteristics, and interference effects on UAV telemetry performance (Heydərov & Əzizullayev, 2024; Rustamov et al., 2025).

The system architecture is shown in the following diagram, illustrating the interaction between the flight controller, telemetry modules, antennas, and communication interfaces.

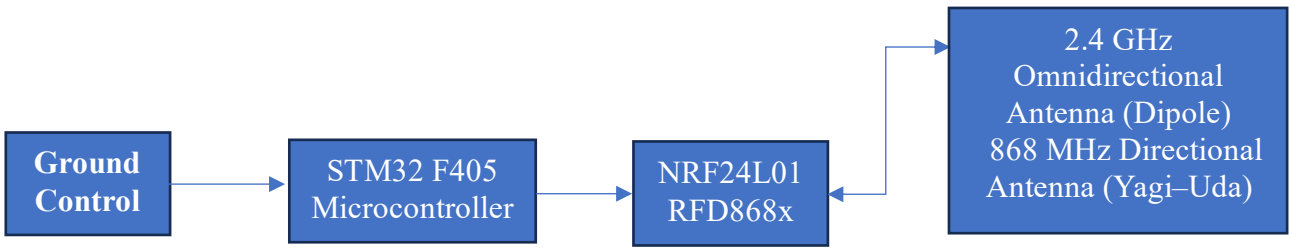

Figure 1
Functional-structural block diagram of the transmitter section of the UAV telemetry system

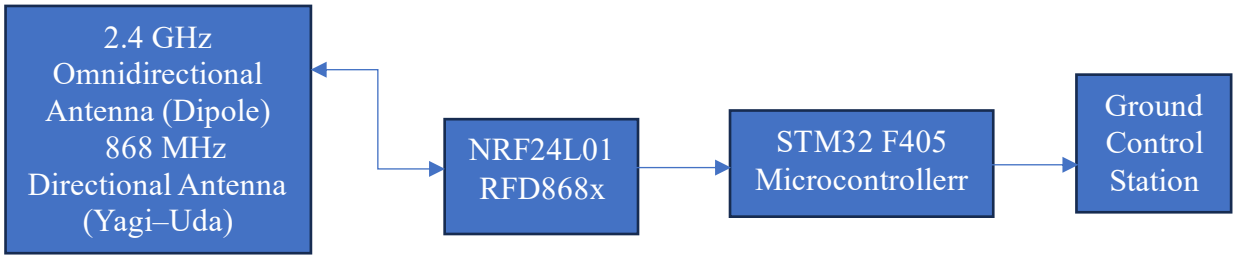

Figure 2
Functional-structural block diagram of the receiver section of the UAV telemetry system

Figures 1 and 2 show the functional block diagrams of the transmitter and receiver sections of the UAV telemetry system and present its overall communication architecture. In this structure, the STM32 F405 microcontroller acts as the central control unit, processing sensor and control data and transmitting them to the NRF24L01 or RFD868x telemetry modules via UART and SPI interfaces.

The signal is then radiated through the antenna, received on the opposite side, demodulated by the telemetry module, and forwarded to the microcontroller for further processing. Data exchange is carried out through SPI, UART, and I2C protocols, while an FHSS-based frequency hopping mechanism is applied to improve resistance to interference. As a result, the proposed architecture enhances transmission reliability and communication stability under radio-electronic warfare conditions.

Flight Controller Architecture. In this study, the flight controller was designed in the EasyEDA environment. Its architecture includes the microcontroller core, power management unit, sensor interfaces, and communication ports for telemetry module integration. The microcontroller performs flight control, sensor data acquisition and processing, and telemetry packet generation, while UART and SPI interfaces support telemetry communication. Stable system operation is ensured by regulated 5 V and 3.3 V power lines.

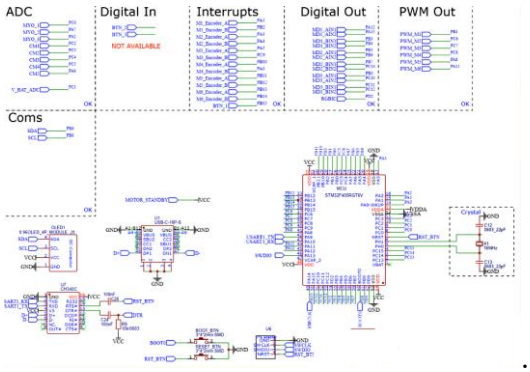

Figure 3
Electronic circuit schematic of the STM32 F405-based flight controller developed in the EasyEDA design environment

Figure 3 presents the electronic schematic of the flight controller developed on the basis of the **STM32 F405** microcontroller. The schematic includes the power supply section, input/output interfaces, sensor connections, and communication blocks. Acting as the main control unit, the microcontroller performs sensor data processing, PWM signal generation, and telemetry data transmission.

Within the system architecture, telemetry module integration is implemented through SPI and UART interfaces, which enables communication in different frequency bands, namely 2.4 GHz and 868 MHz. The presented architecture was optimized to improve communication robustness and ensure telemetry channel reliability under radio-electronic warfare conditions.

Telemetry Module Integration. Two telemetry configurations were integrated into the STM32 F405-based flight controller for comparative evaluation. The NRF24L01 module operating at 2.4 GHz was used for short-range low-latency communication, while the RFD868x module operating at 868 MHz was applied for more stable long-range telemetry transmission. Both modules were evaluated under identical conditions at 50 m, 100 m, 200 m, and 500 m to assess link reliability and signal behavior across different operating ranges.

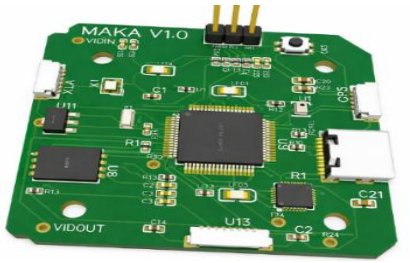

Figure 4
3D PCB model of the STM32 F405-based flight controller (dimensions: 4 × 4 cm)

Figure 4 illustrates the 3D PCB model of the flight controller based on the STM32 F405 microcontroller. The board integrates the power supply unit, sensor interfaces, and telemetry connection components within a compact architecture. Its small dimensions (4 × 4 cm) make it suitable for UAV applications, where low weight, compactness, and integration efficiency are critical design requirements (Sahibcanov & Azizullayev, 2024).

3.2. Communication Modules and Frequency Hopping Algorithm. To increase telemetry channel resilience under radio-electronic warfare conditions, a frequency hopping approach was applied. The algorithm selects operating channels according to a pseudo-random sequence from a predefined frequency set, reducing the risk of fixed-frequency suppression and improving communication reliability under intentional interference. Its effectiveness was evaluated using RSSI, SNR, effective SNR, SINR, BER, and latency indicators (Rustamov et al., 2025).

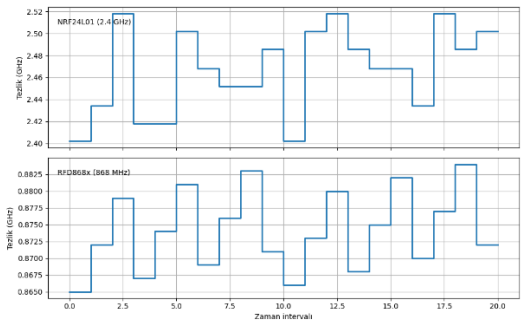

Figure 5
Pseudo-random FHSS frequency hopping sequence for NRF24L01 (2.4 GHz) and RFD868x (868 MHz) telemetry modules

Figure 5 shows the FHSS frequency hopping sequences of the NRF24L01 and RFD868x modules in separate panels. At each time interval, the operating channel changes according to the predefined hopping sequence, which reduces the risk of continuous blocking on a fixed frequency. This figure clearly illustrates the practical implementation of FHSS in both telemetry modules and its contribution to maintaining communication continuity under interference conditions.

User Interface for Real-Time Monitoring of UAV Telemetry Parameters. The developed user interface for real-time monitoring of UAV telemetry parameters is presented in Figure 6. This interface was designed to visualize the main measured communication indicators and to support comparative analysis of NRF24L01 and RFD868x telemetry configurations under radio-electronic warfare conditions.

Figure 6

User interface for real-time monitoring of UAV telemetry parameters

Figure 6 presents the user interface developed for real-time monitoring of UAV telemetry parameters. The interface displays the main communication indicators, including RSSI, SNR, SINR, BER, latency, and path loss, and provides a comparative view of NRF24L01 and RFD868x module performance. It also visualizes the distance-dependent signal quality trend and the telemetry data flow from UAV sensors to the ground station. This interface supports experimental analysis by making link degradation, interference influence, and module-level performance differences easier to observe under radio-electronic warfare conditions.

3.3. Mathematical Performance Models. In this study, the resilience of the UAV telemetry channel under radio-electronic warfare conditions was evaluated using key mathematical performance indicators. The analysis included distance-dependent path loss, received signal strength, SNR, effective SNR, SINR, BER, and latency, which characterize signal propagation, interference impact, transmission reliability, and communication delay. These models provide a quantitative basis for comparing the NRF24L01 and RFD868x modules under normal and interference-affected conditions. They also make it possible to relate telemetry reliability to operating frequency, transmission distance, and radio-electronic interference effects, in line with recent studies on UAV communication security and jamming detection (Yang et al., 2025; Aich et al., 2025).

Path Loss Model. One of the most important parameters in wireless communication channels is Path Loss (PL), which describes the attenuation of the transmitted signal during propagation from the transmitter to the receiver. This attenuation is mainly determined by the communication distance and the characteristics of the surrounding environment, including obstacles, reflections, and shadowing effects. In UAV telemetry systems operating under radio-electronic warfare conditions, accurate path loss modeling is essential for assessing signal degradation, link stability, and overall communication reliability (Heydərov & Əzizullayev, 2024; Rustamov et al., 2025).

The logarithmic distance path loss model can be expressed as:

$$PL(d) = PL(d_0) + 10n\log_{10}\left(\frac{d}{d_0}\right) + X_\sigma \qquad (1)$$

where:
- $PL(d)$- path loss at distance d, dB;
- $PL(d_0)$- path loss at reference distance d_0, dB;
- n- path loss exponent depending on the propagation environment;
- d- separation distance between transmitter and receiver, m;
- d_0- reference distance, m;
- X_σ- shadowing component representing random signal variations, dB.

In the case of free-space propagation, the path loss can be calculated using the well-known free-space model:

$$PL_{FS}(d) = 20\log_{10}(d) + 20\log_{10}(f) + 32.44 \qquad (2)$$

where:
- d- distance between transmitter and receiver, km;
- f- carrier frequency, MHz.

The presented models serve as a fundamental basis for analyzing signal attenuation over distance and enable the comparison of theoretical predictions with experimental results obtained for different telemetry modules and operating conditions.

Received Signal Strength Model. The received signal power is determined by the transmitter power, antenna gains, and propagation losses in the communication channel. In general, the received signal power can be expressed as

$$P_r = P_t + G_t + G_r - PL(d) - L_s \qquad (3)$$

where:
- P_r- received signal power, dBm;
- P_t- transmitted power, dBm;
- G_t- gain of the transmitting antenna, dBi;
- G_r- gain of the receiving antenna, dBi;
- $PL(d)$- path loss at distance d, dB;
- L_s- additional system losses, dB.

In practical experiments, this parameter is often associated with the Received Signal Strength Indicator (RSSI). RSSI represents the signal level measured directly by the receiver module and, in many cases, can be approximated by the received power:

$$RSSI \approx P_r \qquad (4)$$

This relationship makes it possible to compare the measured values obtained from telemetry modules with the theoretically estimated received signal level. As a result, RSSI serves as an important practical indicator for assessing signal quality and validating the propagation behavior of the telemetry channel under different operating conditions (Rustamov et al., 2025; Rüstəmov et al., 2024).

Signal-to-Noise Ratio Model. One of the principal indicators of communication quality in telemetry systems is the signal-to-noise ratio (SNR). This parameter expresses the ratio between the received useful signal power and the noise power present in the communication channel. In its general form, SNR can be written as

$$SNR = \frac{P_r}{N} \qquad (5)$$

where P_r denotes the received signal power and N represents the noise power.

In logarithmic form, which is more convenient for practical analysis in wireless communication systems, the relationship can be expressed as

$$SNR_{dB} = P_r - N_{dBm} \qquad (6)$$

where:
P_r- received signal power;
N- noise power;
N_{dBm}- noise level expressed in dBm.
A higher SNR value indicates that the useful signal is more dominant than the background noise, which directly contributes to more reliable data transmission, lower error probability, and improved telemetry link stability. Therefore, SNR is considered one of the key parameters for evaluating the quality of UAV telemetry channels under both normal and interference-affected operating conditions.

Under radio-electronic warfare conditions, the telemetry channel is affected by both background noise and intentional electromagnetic interference. Therefore, conventional SNR alone is not sufficient for evaluating channel quality. Effective SNR and SINR provide a more complete assessment by including the interference component in the communication model (Aich et al., 2025; Yang et al., 2025). In this study, interference is modeled as an additional degradation factor that reduces the nominal SNR.

In this case, the effective signal-to-noise ratio can be expressed as

$$SNR_{\text{eff}} = SNR - J \tag{7}$$

where:
SNR_{eff}- effective signal-to-noise ratio under radio-electronic interference, dB;
SNR- nominal signal-to-noise ratio, dB;
J- equivalent interference-induced energy loss or degradation level, dB.
Equation (7) provides a simplified yet practical representation of interference influence and is useful for comparing telemetry channel behavior under normal and interference-affected conditions. However, when the interference signal is treated explicitly as an additional energy component in the channel, a more accurate characterization of communication quality is obtained through the signal-to-interference-plus-noise ratio (Henry et al., 2024; Kumar & Chaudhary, 2024).

In general form, SINR can be written as

$$SINR = \frac{P_r}{N + I} \tag{8}$$

where:
P_r- received useful signal power;
N- noise power;
I- interference power.
Equation (8) shows that the quality of the received signal decreases not only with increasing noise power but also with increasing interference power. As the interference component increases, the denominator of the expression becomes larger, which leads to a corresponding degradation in the effective quality of the telemetry channel. Therefore, both SNR_eff and SINR are essential parameters for evaluating telemetry link robustness in environments affected by intentional electromagnetic interference (Zidane et al., 2024; Aich et al., 2025).

Logarithmic SINR Representation and BER Model. In telecommunications and radiophysics literature, the signal-to-interference-plus-noise ratio (SINR) is commonly expressed on a logarithmic scale, i.e., in decibels. In this form, it can be written as

$$SINR_{dB} = 10\log_{10}\left(\frac{P_r}{N + I}\right) \tag{9}$$

If P_r, N, and $I$are expressed in linear power units, Equation (9) can be applied directly. However, when these quantities are represented in dBm or dB units, the expression may be rewritten in the following equivalent form:

$$SINR_{dB} = P_r^{(dBm)} - 10\log_{10}(N + I) \qquad (10)$$

where $P_r^{(dBm)}$denotes the received signal power expressed in dBm.

Thus, while SNR_{eff}provides a simplified and practical estimate of interference-related signal degradation, **SINR** offers a more rigorous description of the actual energy state of the communication channel by jointly accounting for both noise and interference components. For this reason, the combined use of $SNR_{\text{eff}}$and $SINR$is particularly suitable for the interpretation of experimental results obtained under radio-electronic warfare conditions.

Bit Error Rate Model. One of the principal parameters used to characterize the reliability of a telemetry system is the **Bit Error Rate (BER)**. This indicator represents the proportion of incorrectly received bits within the total number of transmitted bits and can be expressed as

$$BER = \frac{N_{err}}{N_{tot}} \qquad (11)$$

where:
N_{err}- number of erroneously received bits;
N_{tot}- total number of transmitted bits.
In communication theory, BER is often related to SNR or SINR. For example, for binary modulation schemes, a commonly used approximation is given by

$$BER \approx Q\left(\sqrt{2\frac{E_b}{N_0}}\right) \qquad (12)$$

where:
$Q(\cdot)$- Q-function;
E_b/N_0- ratio of bit energy to noise spectral density.
In the experimental part of this study, BER was evaluated in a practical manner based on Equation (11), using the ratio of erroneous bits to the total number of transmitted bits. This approach enabled a direct comparison of the transmission reliability of the NRF24L01 and RFD868x modules under both normal and interference-affected operating conditions (Azizullayev, 2025; Rustamov et al., 2024).

Latency Model. In telemetry systems, the timely delivery of information is of critical importance; therefore, latency is considered one of the key performance indicators of communication quality. In general, the total delay can be represented as the sum of several contributing components:

$$T_{lat} = T_{proc} + T_{queue} + T_{tx} + T_{prop} \qquad (13)$$

where:
T_{lat}- total latency;
T_{proc}- processing delay inside the microcontroller or communication module;
T_{queue}- packet waiting time in the transmission queue;
T_{tx}- transmission time;

T_{prop}- signal propagation time.
The transmission time depends on the packet length and the channel bit rate, and can be expressed as

$$T_{tx} = \frac{L_{pkt}}{R_b} \quad (14)$$

where:
L_{pkt}- packet length, bits;
R_b- bit rate, bit/s.
If the propagation component is evaluated separately, it can be written as

$$T_{prop} = \frac{d}{v} \quad (15)$$

where:
d- transmission distance;
v- propagation velocity of the electromagnetic wave (approximately 3×10^8m/s).
These expressions provide the basis for the comparative analysis of communication delay across different distances and telemetry modules. In the present study, the latency model was used to assess how transmission distance, module characteristics, and interference conditions influence the real-time performance of the NRF24L01 and RFD868x telemetry links (Azizullayev, 2025; Rustamov et al., 2025).

Packet Transmission Reliability Model. In addition to signal quality indicators, the reliability of a telemetry channel can also be evaluated using the packet delivery ratio (PDR) and the packet loss ratio (PLR). The packet delivery ratio represents the proportion of successfully received packets to the total number of transmitted packets and can be expressed as

$$PDR = \frac{N_{rx}}{N_{tx}} \quad (16)$$

where:
N_{rx}- number of received packets;
N_{tx}- number of transmitted packets.
The packet loss ratio can then be calculated as

$$PLR = 1 - PDR \quad (17)$$

These parameters are useful for evaluating telemetry reliability under radio-electronic interference, where packet corruption, link interruption, and transmission instability may occur. In this study, PDR and PLR were used as complementary indicators of operational robustness under different distance and interference scenarios (Zidane et al., 2024; Yang et al., 2025).

Overall, the mathematical models provide a unified framework for assessing telemetry performance in terms of signal attenuation, received power, channel quality, transmission reliability, and latency. Path loss, RSSI, SNR, effective SNR, SINR, BER, PDR, PLR, and latency were jointly used to analyze the communication behavior of the NRF24L01 and RFD868x modules under normal and interference-affected conditions (Rustamov et al., 2025; Zheng et al., 2023).

3.4. Validation and Evaluation Methodology. To validate the proposed UAV telemetry communication model, a simulation-supported analytical evaluation methodology was applied. The validation was based on the mathematical models presented above and was used to compare the

NRF24L01 and RFD868x modules under identical operating conditions (Rustamov et al., 2025; Zheng et al., 2023).

The evaluation was conducted at four distances: 50 m, 100 m, 200 m, and 500 m. For each distance, two scenarios were considered: normal communication conditions and radio-electronic warfare conditions. In the interference scenario, an additional jamming-related degradation component was included in the analytical model to assess telemetry link stability (Zidane et al., 2024; Aich et al., 2025).

The main evaluation parameters were RSSI, SNR, effective SNR, SINR, BER, latency, path loss, PDR, and PLR. The same distance values, channel assumptions, and performance indicators were applied to both telemetry modules to ensure objective comparison. The obtained results were visualized using the Matplotlib library in Python, allowing the distance-dependent behavior of the telemetry channel to be analyzed under normal and interference-affected conditions.

Results

The obtained results show that increasing the transmission distance from 50 m to 500 m caused higher path loss and gradual degradation of telemetry channel quality. For both modules, RSSI, SNR, effective SNR, and SINR decreased with distance, while BER and latency increased. This tendency became more pronounced under radio-electronic warfare conditions.

The NRF24L01 module demonstrated better latency at short distances, especially at 50 m and 100 m, which makes it suitable for short-range telemetry and control applications. However, due to operation in the 2.4 GHz band, its signal quality degraded more rapidly at longer distances and under interference conditions. The RFD868x module showed more stable performance in the 200-500 m range. Its 868 MHz operating frequency provided lower path loss, stronger RSSI, higher SNR/SINR values, and lower BER compared with the NRF24L01 module. This confirms its advantage for longer-range telemetry communication under interference-affected conditions. The graphical results also support these findings. Path loss increased with distance, RSSI and SNR decreased, and BER and latency increased under radio-electronic warfare conditions. Antenna analysis further showed that the 2.4 GHz omnidirectional antenna is more suitable for flexible short-range communication, whereas the 868 MHz directional antenna improves received signal strength and link stability at longer distances. Overall, the results indicate that NRF24L01 is preferable for short-range low-latency telemetry, while RFD868x provides higher reliability and stronger interference resistance over longer distances.

Table 1
Comparative performance indicators of the NRF24L01 module under normal communication conditions

Distance, m	Path Loss, dB (1-2)	RSSI, dBm (3-4)	SNR, dB (5-6)	Effective SNR, dB (7)	BER (11)	Latency, ms (13-15)
50	75	-52	38	38	0.0002	12
100	81	-58	32	32	0.0007	14
200	87	-66	24	24	0.0025	17
500	95	-79	11	11	0.0120	23

Table 1 presents the performance indicators of the NRF24L01 module under normal communication conditions. The results show that as the transmission distance increases, path loss rises, while RSSI and SNR decrease. In parallel, BER and latency gradually increase, indicating reduced communication quality and transmission reliability over longer distances.

Table 2
Performance indicators of the NRF24L01 module under radio-electronic warfare conditions

Distance, m	Path Loss, dB (1-2)	RSSI, dBm (3-4)	SNR, dB (5-6)	Effective SNR, dB (7)	SINR, dB (8-10)	BER (11)	Latency, ms (13-15)
50	75	-55	35	27	24	0.0015	16
100	81	-62	28	20	17	0.0040	19
200	87	-72	18	10	8	0.0180	25
500	95	-88	5	-3	-6	0.0850	34

Table 2 summarizes the performance indicators of the NRF24L01 module under radio-electronic warfare conditions. Compared with normal communication conditions, the results show a noticeable degradation in signal quality, reflected in lower RSSI, SNR, effective SNR, and SINR values. At the same time, BER and latency increase with distance, indicating reduced communication reliability under interference-affected operating conditions.

Table 3
Performance indicators of the RFD868x module under normal communication conditions

Distance, m	Path Loss, dB (1-2)	RSSI, dBm (3-4)	SNR, dB (5-6)	Effective SNR, dB (7)	BER (11)	Latency, ms (13-15)
50	66	-46	41	41	0.0001	28
100	72	-51	36	36	0.0003	31
200	78	-58	29	29	0.0010	36
500	86	-69	18	18	0.0055	47

Table 3 presents the performance indicators of the RFD868x module under normal communication conditions. The results indicate that, due to its lower operating frequency and more stable propagation characteristics, the RFD868x module demonstrates improved performance over longer distances compared with the NRF24L01 module. This is reflected in higher RSSI and SNR values, as well as lower BER, confirming the suitability of sub-GHz communication for extended-range telemetry applications.

Table 4
Performance indicators of the RFD868x module under radio-electronic warfare conditions

Distance, m	Path Loss, dB (1-2)	RSSI, dBm (3-4)	SNR, dB (5-6)	Effective SNR, dB (7)	SINR, dB (8-10)	BER (11)	Latency, ms (13-15)
50	66	-49	38	31	28	0.0008	32
100	72	-55	32	25	22	0.0018	36
200	78	-63	24	17	14	0.0065	43
500	86	-76	11	4	1	0.0280	58

Table 4 shows that the RFD868x module maintains stronger performance under radio-electronic warfare conditions, especially in the 200-500 m range. Higher RSSI, effective SNR, and SINR values, together with lower BER, confirm the greater resilience of the 868 MHz telemetry link.

Overall, the results indicate that increasing distance raises path loss and reduces RSSI and SNR for both modules. Under interference conditions, this degradation becomes stronger, leading to lower

effective SNR/SINR, higher BER, and increased latency. NRF24L01 provides lower latency at shorter ranges, whereas RFD868x ensures more stable long-range communication.

For graphical analysis, the obtained data were visualized using the Matplotlib library in the Python environment. The plots illustrate the distance-dependent variation of the main telemetry channel parameters under normal and radio-electronic warfare conditions.

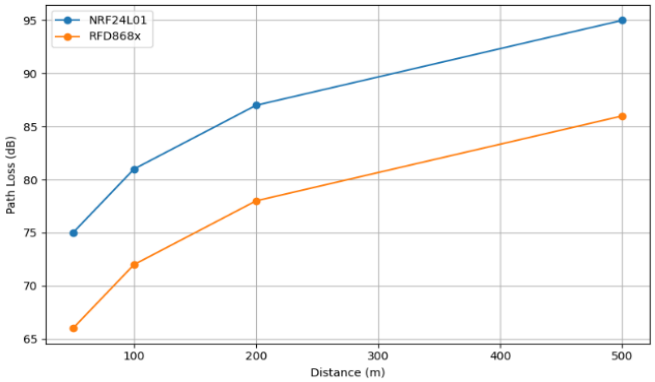

Figure 7
Graph of the dependence of Path Loss on distance

Figure 7 shows the distance-dependent variation of path loss calculated using Equations (1) and (2). Path loss increases logarithmically with distance for both modules. Higher values are observed for the NRF24L01 module, while the RFD868x module shows lower attenuation due to its lower operating frequency and antenna characteristics.

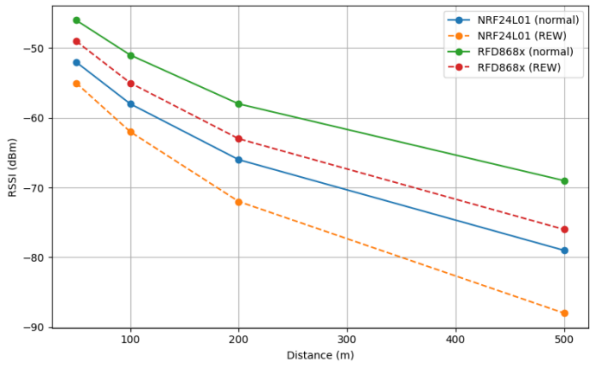

Figure 8
RSSI variation with distance for NRF24L01 and RFD868x modules under normal and REW conditions

Figure 8 shows the distance-dependent variation of RSSI under normal and radio-electronic warfare conditions. The results indicate that RSSI decreases as distance increases, and this degradation becomes more pronounced under interference-affected conditions.

For the NRF24L01 module, the signal level is observed to degrade more rapidly in the presence of REW. In contrast, the RFD868x module preserves a higher RSSI level due to its lower operating frequency range and more favorable propagation characteristics. This, in turn, contributes to improved communication stability over longer distances.

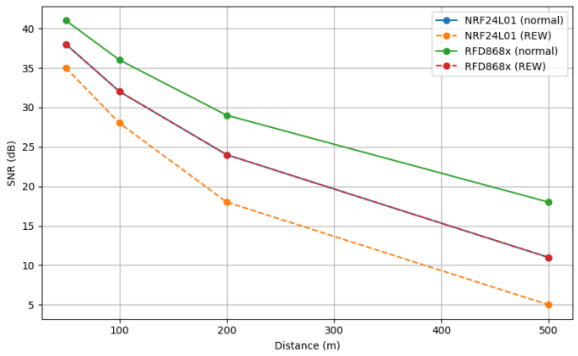

Figure 9
SNR variation with distance for NRF24L01 and RFD868x modules under normal and REW conditions

Figure 9 shows the distance-dependent variation of SNR under normal and radio-electronic warfare conditions. The results indicate that SNR decreases as distance increases, and this reduction becomes stronger under interference. Compared with NRF24L01, the RFD868x module maintains more stable signal quality over longer distances.

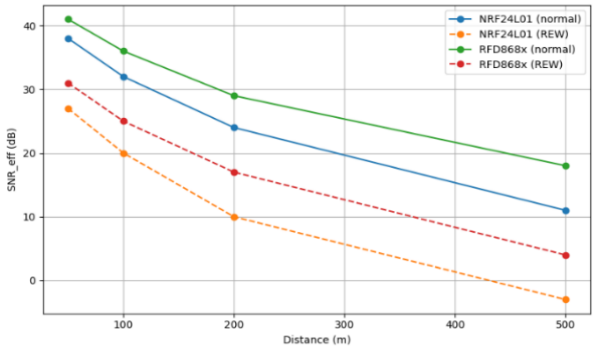

Figure 10
Effective SNR variation with distance for NRF24L01 and RFD868x modules under normal and REW conditions

Figure 10 presents the variation of effective SNR calculated using Equation (7). Under radio-electronic warfare conditions, effective SNR decreases for both modules; however, the degradation is more significant for NRF24L01 at longer distances. In contrast, RFD868x maintains higher effective SNR values, indicating better robustness against interference.

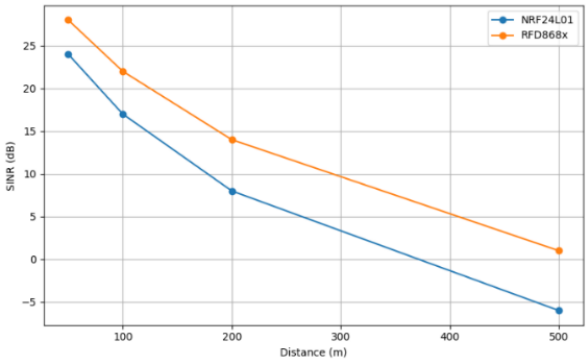

Figure 11
SINR variation with distance for NRF24L01 and RFD868x modules

The graph illustrates the variation of the signal-to-interference-plus-noise ratio (SINR) with distance, calculated on the basis of equations (8) and (9). The results indicate that the influence of the interference signal causes a significant reduction in SINR. For the NRF24L01 module, the SINR falls to negative values at longer distances, which leads to unstable communication performance. In contrast, the RFD868x module preserves a higher SINR level and therefore provides more reliable communication.

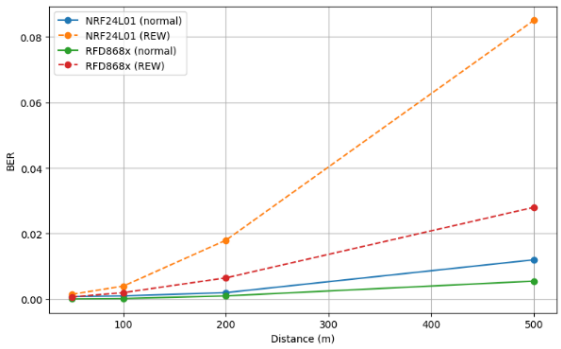

Figure 12
BER variation with distance for NRF24L01 and RFD868x modules under normal and REW conditions

Figure 12 shows the variation of BER with distance under normal and radio-electronic warfare conditions. BER increases as distance grows, and this increase becomes more significant under interference. Compared with NRF24L01, the RFD868x module provides lower BER values, indicating more reliable data transmission.

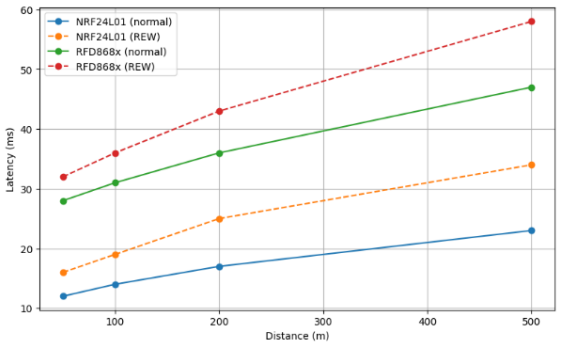

Figure 13
Latency variation with distance for NRF24L01 and RFD868x modules under normal and REW conditions

Figure 13 shows the distance-dependent variation of latency based on Equations (12)-(14). Latency increases with distance for both modules. Although NRF24L01 provides lower latency at short ranges, its delay becomes more sensitive under REW conditions. In contrast, RFD868x has higher initial latency but maintains more stable long-range communication. The results also confirm that frequency hopping reduces signal degradation and improves telemetry reliability under interference conditions (Rustamov et al., 2025; Rüstəmov et al., 2023).

Analysis of Antenna Radiation Patterns. Telemetry reliability depends not only on the radio module and operating frequency, but also on antenna gain, radiation pattern, and directional energy distribution. Therefore, the 2.4 GHz omnidirectional antenna used with NRF24L01 and the 868 MHz

directional antenna used with RFD868x were comparatively analyzed in terms of their effect on telemetry performance (Nakprasit et al., 2020; Ojaroudi Parchin et al., 2020).

The general model of antenna gain as a function of direction is assumed as follows:

$$G(\theta, \varphi) = G_{\max} F_n(\theta, \varphi) \quad (18)$$

where:
$G(\theta, \varphi)$- antenna gain in the given direction, dBi;
$G_{\max}$- maximum antenna gain, dBi;
$F_n(\theta, \varphi)$- normalized radiation function.
The normalization condition is:

$$0 \leq F_n(\theta, \varphi) \leq 1 \quad (19)$$

The received signal power, taking into account antenna gain and channel loss, can be expressed as:

$$P_r(d) = P_t + G_t(\theta, \varphi) + G_r(\theta, \varphi) - PL(d) - L_s \quad (20)$$

where:
$P_r(d)$- received signal power at distance d, dBm;
P_t- transmitter power, dBm;
G_t, G_r- transmitter and receiver antenna gains, dBi;
$PL(d)$- path loss, dB;
L_s- additional system losses, dB.
The distance-dependent path loss is given, as in the previous section, by:

$$PL(d) = PL(d_0) + 10n\log_{10}\left(\frac{d}{d_0}\right) + X_\sigma \quad (21)$$

and for free-space conditions:

$$PL_{FS}(d) = 20\log_{10}(d) + 20\log_{10}(f) + 32.44 \quad (22)$$

where f is the carrier frequency, MHz; and d is the distance, km.

As follows from equation (21), the path loss increases with increasing frequency. Therefore, for the NRF24L01 module operating in the 2.4 GHz band, the attenuation at the same distance is higher than that of the RFD868x module operating in the 868 MHz band. This difference is consistent with the previously obtained Path Loss, RSSI, and SNR results.

The signal-to-noise ratio can be related to antenna gain and received signal power as follows:

$$SNR_{dB} = P_r - N \quad (23)$$

Under radio-electronic warfare (REW) conditions, the effective signal-to-noise ratio is:

$$SNR_{eff} = SNR - J \quad (24)$$

and the signal-to-interference-plus-noise ratio is:

$$SINR = 10\log_{10}\left(\frac{P_r}{N + I}\right) \quad (25)$$

where:
N- noise power;
J- equivalent loss caused by interference, dB;
I- interference signal power.
The relationship between the **BER** indicator and channel quality can generally be expressed as:

$$BER = f(SNR_{eff}, SINR) \qquad (26)$$

that is, as SNR_{eff} and $SINR$ decrease, the probability of bit error increases.

For the NRF24L01 module, an omnidirectional antenna operating in the 2.4 GHz band is considered. The omnidirectional antenna intended for the NRF24L01 module provides a relatively uniform distribution of energy in the horizontal plane. This characteristic makes it suitable for multidirectional communication over short and medium distances.

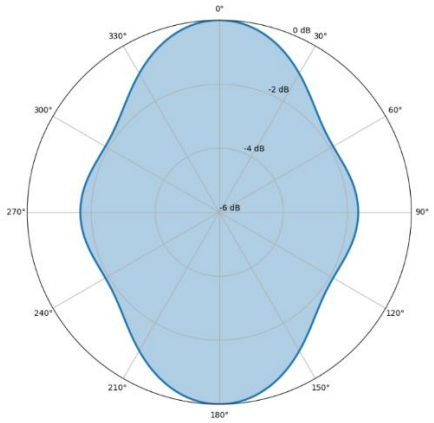

Figure 14
Theoretical radiation pattern of the omnidirectional antenna for the NRF24L01 module in the 2.4 GHz band

Figure 14 shows that the omnidirectional 2.4 GHz antenna enables the NRF24L01 module to maintain stable communication at short distances, particularly at 50 m and 100 m. However, at 200 m and 500 m, signal quality degrades more rapidly due to higher path loss and limited directional gain. In contrast, the 868 MHz directional antenna used with the RFD868x module concentrates energy toward the main lobe, improving received signal strength and long-range telemetry performance.

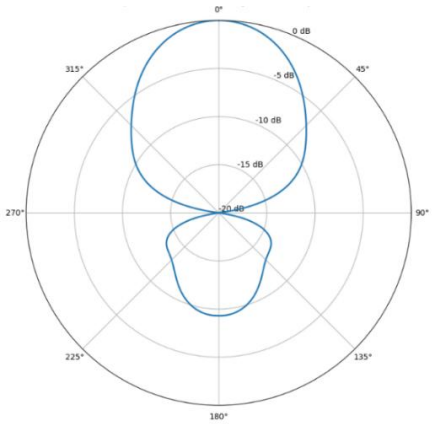

Figure 15
Theoretical radiation pattern of the directional antenna for the RFD868x module in the 868 MHz band

Figure 15 shows that the directional antenna increases received signal power by concentrating radiation toward the main lobe. Together with the lower 868 MHz operating frequency, this improves the RFD868x module's performance at 50 m, 100 m, 200 m, and 500 m. The obtained RSSI and SNR values confirm a higher signal level and more stable communication compared with the NRF24L01 module. Correlation between Antenna Patterns and Telemetry Results. The antenna radiation patterns are consistent with the previously presented performance graphs, where improved directional gain leads to higher received signal strength, better signal quality, and enhanced link stability, particularly at longer distances.

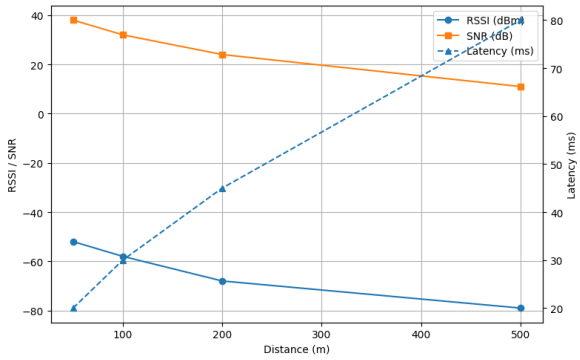

Figure 16
Distance-dependent variation of the main communication parameters for the NRF24L01 module in the 2.4 GHz band

The graph presents the distance-dependent variation of RSSI, SNR, and latency for the NRF24L01 module in the 2.4 GHz band. As can be seen, with increasing distance, the RSSI and SNR values decrease, whereas the latency increases. This confirms that, at longer distances, the use of an omnidirectional antenna together with a higher frequency band leads to greater signal attenuation.

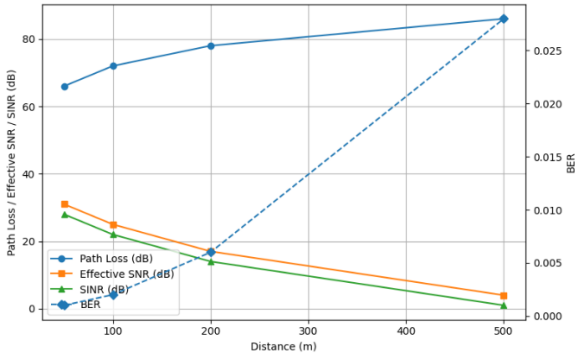

Figure 17
Distance-dependent variation of Path Loss, Effective SNR, SINR, and BER for the RFD868x module

Figure 17 illustrates the distance-dependent variation of path loss, effective SNR, SINR, and BER for the RFD868x module. As distance increases, path loss and BER rise, while effective SNR and SINR decrease. However, the 868 MHz band and directional antenna help preserve signal stability and maintain a lower error probability over longer distances.

Overall, the antenna radiation analysis confirms that the 2.4 GHz omnidirectional antenna used with NRF24L01 is suitable for flexible short-range communication, while the 868 MHz directional antenna used with RFD868x provides stronger received signal level, higher SNR, and lower BER over longer distances. These results are consistent with Equations (19)-(25) and the obtained findings.

Results and Discussion

The results show that UAV telemetry reliability under radio-electronic warfare conditions is mainly affected by operating frequency, propagation loss, antenna characteristics, interference level, and FHSS performance. As distance increased from 50 m to 500 m, path loss and latency increased, while RSSI, SNR, effective SNR, and SINR decreased, confirming the influence of distance and interference on link quality (Aghayev et al., 2025; Rustamov et al., 2025). The NRF24L01 module at 2.4 GHz showed lower latency at short distances, but its performance degraded more rapidly under attenuation and interference. In contrast, the RFD868x module at 868 MHz maintained stronger RSSI, SNR, and SINR values, making it more suitable for longer-range and interference-affected telemetry links (Zidane et al., 2024; Yang et al., 2025). Antenna analysis also confirmed that the 2.4 GHz omnidirectional antenna is suitable for flexible short-range coverage, whereas the 868 MHz directional antenna improves received signal strength over longer distances. Overall, FHSS increases telemetry resilience, but its effectiveness depends on frequency band, antenna configuration, and module selection (Rüstəmov et al., 2023; Rustamov, Gasanov, Azizullayev, & Hasanli, 2025).

The study showed that the application of the Frequency-Hopping Spread Spectrum (FHSS) method improves the robustness of UAV telemetry channels under radio-electronic warfare conditions and reduces the risk of fixed-frequency jamming. The STM32 F405-based flight controller designed in the EasyEDA environment provided a practical hardware platform for integrating and comparing different telemetry modules. The comparative analysis demonstrated that the NRF24L01 module operating in the 2.4 GHz band is more suitable for short-range, low-latency telemetry communication. However, its signal quality degrades more rapidly as distance and interference increase. In contrast, the RFD868x module operating in the 868 MHz band provided more stable communication over longer distances, especially in the 200-500 m range, due to lower path loss, stronger received signal level, and lower bit error rate. The obtained results confirmed that increasing distance leads to higher path loss and latency, while RSSI, SNR, effective SNR, and SINR decrease. Under interference-affected conditions, BER increases and telemetry reliability decreases. Antenna radiation pattern analysis also showed that the 2.4 GHz omnidirectional antenna is effective for flexible short-range communication, whereas the 868 MHz directional antenna improves signal stability over longer distances.

The main novelty of the study is the integrated evaluation of an FHSS-based telemetry approach, STM32 F405 flight controller architecture, two different telemetry modules, and antenna characteristics within a single comparative framework. Overall, the proposed approach can be considered a practical solution for improving UAV telemetry reliability under radio-electronic warfare conditions. Future work will focus on field-based validation under different jamming intensities, flight altitudes, and antenna alignment conditions.

References

1. Aghayev, F., Rustamov, A., Binnatov, M., Azizullayev, M., & Sahibcanov, A. (2025). Intervention methods in control and communication systems of unmanned aerial vehicles: Analysis and evaluation of signal quality. *Security & Defense, 1*, 71–85. https://doi.org/10.70265/FKJC9739
2. Aich, N., Oubrahim, Z., Ait Talount, H., & Abbou, A. (2025). Bi-scale Mahalanobis detection for reactive jamming in UAV OFDM links. *Future Internet, 17*(10), 474. https://doi.org/10.3390/fi17100474
3. Azizullayev, M. G. (2025). Analytical and mathematical modeling of long-range UAV telemetry systems under electromagnetic interference. *Engineer International Scientific Journal, 3*(4). https://doi.org/10.56143/3pang560

4. Azizullayev, M. G., & Nematzade, R. G. (2025). Experimental measurement and mathematical modeling of UAV telemetry channel behavior under radio-electronic warfare. *Engineer International Scientific Journal, 3*(4), 60–64. https://doi.org/10.56143/jqj9n976
5. Ghouz, H. H. M., Abo Sree, M. F., & Ibrahim, M. A. (2020). Novel wideband microstrip monopole antenna designs for WiFi/LTE/WiMax devices. *IEEE Access, 8*, 9532–9539. https://doi.org/10.1109/ACCESS.2019.2963644
6. Henry, J. K. A., Narayanan, R. M., & Singla, P. (2024). Radar cross-section modeling of space debris. In E. Blasch, F. Darema, & A. Aved (Eds.), *Dynamic Data Driven Applications Systems: DDDAS 2022* (Lecture Notes in Computer Science, Vol. 13984). Springer. https://doi.org/10.1007/978-3-031-52670-1_8
7. Heydərov, N., & Əzizullayev, M. Q. (2024). Aerodinamik parametrlərin və aerodinamik qüvvə əmsalının təyinedilmə metodu. *Hərbi Bilik, 2*, 23–30.
8. Kumar, N., & Chaudhary, A. (2024). Surveying cybersecurity vulnerabilities and countermeasures for enhancing UAV security. *Computer Networks, 252*, Article 110695. https://doi.org/10.1016/j.comnet.2024.110695
9. Nakprasit, K., Sakonkanapong, A., & Phongcharoenpanich, C. (2020). Elliptical ring antenna excited by circular disc monopole for UWB communications. *International Journal of Antennas and Propagation, 2020*, Article 8707182. https://doi.org/10.1155/2020/8707182
10. Ojaroudi Parchin, N., Jahanbakhsh Basherlou, H., Al-Yasir, Y. I. A., Abdulkhalek, A. M., Patwary, M., & Abd-Alhameed, R. A. (2020). A new CPW-fed diversity antenna for MIMO 5G smartphones. *Electronics, 9*(2), Article 261. https://doi.org/10.3390/electronics9020261
11. Rustamov, A. R., Gasanov, A. G., & Azizullayev, M. G. (2024). Analysis of modules and systems used in effective control of UAVs in radio electronic combat environment. In *Suchasni napriamy rozvytku informatsiino-komunikatsiinykh tekhnolohii ta zasobiv upravlinnia: Proceedings of the 14th International Scientific and Technical Conference* (Vol. 1, pp. 47–48).
12. Rustamov, A. R., Gasanov, A. G., Azizullayev, M. G., & Hasanli, R. A. (2025). Experimental study of the resistance of telemetry and communication systems of unmanned aerial vehicles in radio electronic warfare environment in laboratory and field conditions. In *Problems of Informatization: Proceedings of the 13th International Scientific and Technical Conference* (Vol. 2, p. 2).
13. Rustamov, A. R., Gasanov, A. G., Azizullayev, M. G., & Hasanli, R. A. (2025). Pluto software defined radio based adaptive frequency spread system in telemetry communication of unmanned aircraft in radio electronic warfare conditions. In *Problems of Informatization: Proceedings of the 13th International Scientific and Technical Conference* (Vol. 1, pp. 64–65).
14. Rustamov, A. R., Gasanov, A. G., Azizullayev, M. G., & Hasanli, R. A. (2025). Radio analysis of telemetry indicators of unmanned aerial vehicles in electronic warfare conditions. In *Problems of Informatization: Proceedings of the 13th International Scientific and Technical Conference* (Vol. 2, pp. 6–7).
15. Rustamov, A. R., Gasanov, A. G., Azizullayev, M. G., & Hasanli, R. A. (2025). Small sized unmanned aerial vehicles signal protection against detection technologies and resilience of telemetry systems. In *Problems of Informatization: Proceedings of the 13th International Scientific and Technical Conference* (Vol. 2, pp. 127–128).
16. Rustamov, A., Azizullayev, M., & Rahimli, V. (2025). Artificial intelligence in naval operations and the enhancement of fleet combat resilience. In *Formation of Innovative Potential of World Science: Proceedings of the X International Scientific and Theoretical Conference* (pp. 97–103).
17. Rustamov, A., Hashimov, E., Muradov, T., Hashimov, R., & Azizullayev, M. (2025). Analysis of antenna system modeling with the help of simulation technology of navigation equipment. *Advanced Information Systems, 9*(2), 36–43. https://doi.org/10.20998/2522-9052.2025.2.05
18. Rüstəmov, Ə. R., Binnətov, M. F., Qurbanov, X., & Əzizullayev, M. Q. (2023). Xüsusi təyinatlı radioelektron vasitələrin təkmilləşdirilməsi ilə etibarlılığın təmin edilməsi. *Milli Təhlükəsizlik və Hərbi Elmlər, 4*(9), 28–35.

19. Rüstəmov, Ə. R., Məmmədzadə, V. M., Məlikov, F. Ə., Həşimov, R. İ., & Əzizullayev, M. Q. (2024). Xəzər dənizində təhlükəsizliyin təminində naviqasiya və hidroqrafiya təminatının rolu. *Hərbi Bilik, 2*, 65–75.
20. Sahibcanov, A. E., & Azizullayev, M. G. (2024, June 7). Schemo-technical solutions for designing national flight cards for UAVs. In *Proceedings of the International Conference on Information Technology Trends Dedicated to the 101st Anniversary of Heydar Aliyev* (pp. 101–106). https://dspace.asoiu.edu.az/jspui/handle/123456789/460
21. Yang, H., Liu, Y., Li, X., Bai, Z., Yang, L., Pan, G., et al. (2025). Physical layer security and covert communication in UAV-ISAC networks: A comprehensive survey. *Journal of King Saud University – Computer and Information Sciences, 37*, 312.
22. Zheng, C., Ge, Y., & Guo, A. (2023). Ultra-wideband technology: Characteristics, applications and challenges. *arXiv*. https://doi.org/10.48550/arXiv.2307.13066
23. Zidane, Y., Silva, J. S., & Tavares, G. (2024). Jamming and spoofing techniques for drone neutralization: An experimental study. *Drones, 8*(12), 743. https://doi.org/10.3390/drones8120743